Exploitation of conserved eukaryotic host cell farnesylation machinery by an F-box effector of *Legionella pneumophila*

Christopher T.D. Price,[1] Tasneem Al-Quadan,[1] Marina Santic,[3] Snake C. Jones,[1] and Yousef Abu Kwaik[1,2]

[1]Department of Microbiology and Immunology, School of Medicine and [2]Department of Biology, University of Louisville, Louisville, KY 40292
[3]Department of Microbiology and Parasitology, University of Rijeka School of Medicine, HR-51000, Rijeka, Croatia

Farnesylation involves covalent linkage of eukaryotic proteins to a lipid moiety to anchor them into membranes, which is essential for the biological function of Ras and other proteins. A large cadre of bacterial effectors is injected into host cells by intravacuolar pathogens through elaborate type III–VII translocation machineries, and many of these effectors are incorporated into the pathogen-containing vacuolar membrane by unknown mechanisms. The Dot/Icm type IV secretion system of *Legionella pneumophila* injects into host cells the F-box effector Ankyrin B (AnkB), which functions as platforms for the docking of polyubiquitinated proteins to the *Legionella*-containing vacuole (LCV) to enable intravacuolar proliferation in macrophages and amoeba. We show that farnesylation of AnkB is indispensable for its anchoring to the cytosolic face of the LCV membrane, for its biological function within macrophages and *Dictyostelium discoideum*, and for intrapulmonary proliferation in mice. Remarkably, the protein farnesyltransferase, RCE-1 (Ras-converting enzyme-1), and isoprenyl cysteine carboxyl methyltransferase host farnesylation enzymes are recruited to the LCV in a Dot/Icm-dependent manner and are essential for the biological function of AnkB. In conclusion, this study shows novel localized recruitment of the host farnesylation machinery and its anchoring of an F-box effector to the LCV membrane, and this is essential for biological function in vitro and in vivo.

CORRESPONDENCE
Yousef Abu Kwaik:
abukwaik@louisville.edu

Abbreviations used: AnkB, Ankyrin B; BAP, bacterial alkaline phosphatase; ICMT, isoprenyl cysteine carboxyl methyltransferase; LCV, *Legionella*-containing vacuole; MOI, multiplicity of infection; PFT, protein farnesyltransferase; PGGT, protein geranylgeranyltransferase I; RNAi, RNA interference.

Exploitation of eukaryotic cellular processes is essential for intracellular proliferation of intracellular microbial pathogens. The Legionnaires' disease–causing bacterium, *Legionella pneumophila*, replicates within alveolar macrophages, causing pneumonia (Isberg et al., 2009). The organism is transmitted to humans from the aquatic environment where *L. pneumophila* replicates within amoeba and ciliates (Molmeret et al., 2005; Franco et al., 2009).

Coevolution and adaptation of *L. pneumophila* to the intracellular lifestyle within amoeba in the aquatic environment is believed to have played a major role in its ability to exploit evolutionarily conserved eukaryotic processes that enable its proliferation within human alveolar macrophages (Molmeret et al., 2005; Franco et al., 2009). Within both evolutionarily distant host cells, *L. pneumophila* evades endocytic fusion and intercepts ER to Golgi vesicle traffic to remodel its phagosome into an ER-derived vacuole (Kagan and Roy, 2002; Molmeret et al., 2005; Shin and Roy, 2008; Isberg et al., 2009). The Dot/Icm type IV secretion system (Segal et al., 1998; Vogel et al., 1998) injects into the host cell a cadre of ~200 effectors to modulate a myriad of cellular processes to reprogram the host cell into a proliferation niche (de Felipe et al., 2008; Shin and Roy, 2008; Isberg et al., 2009). The Ankyrin B (AnkB) effector is injected into the host cell by the Dot/Icm system upon bacterial attachment to the plasma membrane and exploits an evolutionarily conserved eukaryotic machinery within mammalian and protozoan cells (Price et al., 2009).

C.T.D Price and T. Al-Quadan contributed equally to this paper.

The Rockefeller University Press $30.00
J. Exp. Med. Vol. 207 No. 8 1713-1726
www.jem.org/cgi/doi/10.1084/jem.20100771

The Dot/Icm-translocated AnkB effector is a noncanonical F-box protein that harbors two eukaryotic-like Ankyrin domains (ANK) that are thought to be involved in protein–protein interaction and is highly regulated by the growth phase (Al-Khodor et al., 2008, 2010a,b; Habyarimana et al., 2008). The F-box domain of AnkB interacts with the host SKP1 component of the SCF1 ubiquitin ligase complex and functions as a platform for the docking of polyubiquitinated proteins to the *Legionella*-containing vacuole (LCV) membrane within primary human macrophages, the U937 human macrophage cell line, HEK293 cells, *Acanthamoeba polyphaga*, and *Dictyostelium discoideum* (Dorer et al., 2006; Price et al., 2009). The AnkB effector is essential for proliferation of *L. pneumophila* within the two evolutionarily distant hosts, mammalian and protozoan cells, and for intrapulmonary bacterial proliferation and manifestation of pulmonary disease in the mouse model (Al-Khodor et al., 2008; Price et al., 2009). Importantly, the F-box domain as well as the two ankyrin protein–protein interaction domains are all essential for the biological function of AnkB (Al-Khodor et al., 2008; Price et al., 2009, 2010).

Prenylation is a highly conserved posttranslation lipid modification of eukaryotic proteins that confers hydrophobicity on the modified protein and its targeting to membranes (Wright and Philips, 2006). Prenylation is mediated by protein geranylgeranyltransferase I (PGGT), protein farnesyltransferase (PFT), or by Rab geranylgeranyltransferase (Wright and Philips, 2006). This posttranslational modification plays a key role in the functional activity of numerous eukaryotic proteins, including Rab proteins, Ras, G proteins, and protein kinases (Casey et al., 1989; Hancock et al., 1989; Mumby et al., 1990; Yamane et al., 1990; Wang et al., 1992). Prenylation involves the covalent addition of either a 15-carbon farnesyl or a 20-carbon geranylgeranyl isoprenoid moiety at a cysteine residue in a conserved C-terminal tetrapeptide CaaX motif. After farnesylation of the conserved cysteine residue of the CaaX motif, the terminal -aaX tripeptide is often cleaved by the RCE-1 (Ras-converting enzyme-1) protease in the ER membrane (Boyartchuk et al., 1997). Then the C-terminal farnesylated cysteine is methylated by isoprenyl cysteine carboxyl methyltransferase (ICMT; Dai et al., 1998; Bergo et al., 2000).

A myriad of effectors is injected into the host cell by elaborate type III–VII translocation systems of intravacuolar pathogens. Although many injected bacterial effectors are anchored into the pathogen-containing vacuolar membrane of intracellular pathogens, the mechanism of this anchoring is not well understood. Our data show that host cell farnesylation of AnkB anchors it to the membrane of the LCV and that the three host enzymes involved in farnesylation are recruited to the LCV in a Dot/Icm-dependent manner and are essential for the biological function of AnkB, which is novel. Farnesylation of AnkB is indispensable in vivo where the defect in farnesylation results in total attenuation in intrapulmonary proliferation in mice, similar to the genetic ablation of *ankB*.

RESULTS

Localization of ectopically expressed AnkB to the plasma membrane of mammalian cells and *D. discoideum* is mediated by its C-terminal CaaX motif

Microscopic analyses showed that ectopically expressed 3xFlag AnkB in HEK293 cells and in *D. discoideum* exhibits a striking localization at the cell periphery (Fig. 1 A and Fig. S1; Price et al., 2009). In silico analysis of AnkB revealed that the last C-terminal 4 aa residues (^{169}CVLC) constitute a potential eukaryotic CaaX motif. To examine whether localization of AnkB to the cell periphery/plasma membrane was caused by farnesylation, a substitution (cysteine to alanine) mutant allele (*ankB*^{169}*C/A*) was

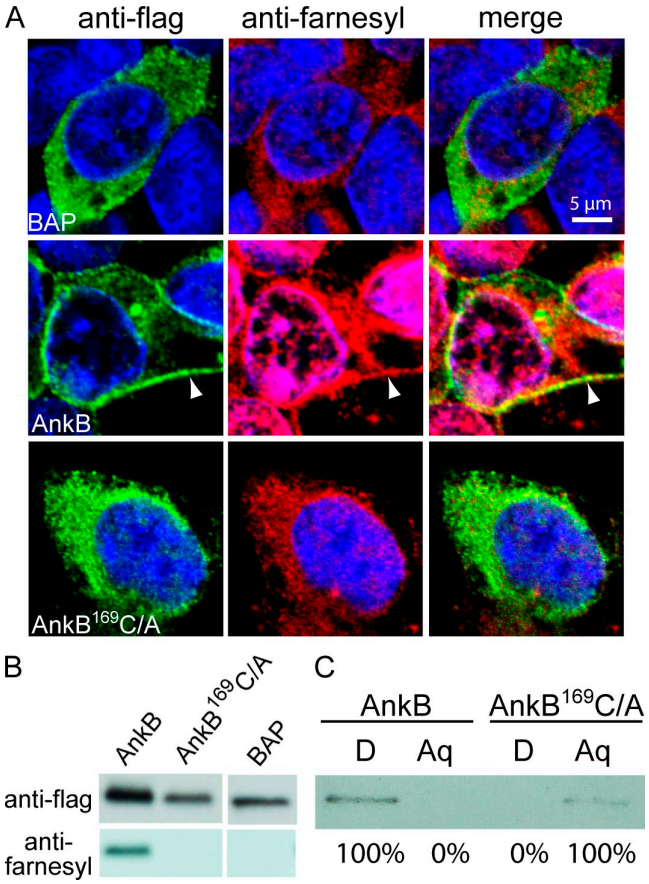

Figure 1. Ectopically expressed 3xFlag AnkB is farnesylated and is targeted to the plasma membrane. (A) Representative confocal microscopy images of cells ectopically expressing 3xFlag-tagged AnkB, AnkB^{169}C/A, and BAP. Green indicates labeling with anti-Flag antibody, whereas red indicates labeling with antifarnesyl antibody, and the nucleus is stained blue (DAPI). The arrowheads indicate strong colocalization of AnkB with farnesylation at the plasma membrane. (B) Transfected HEK293 cells expressing 3xFlag-tagged proteins were lysed, immunoprecipitated with an anti-Flag antibody, and immunoblotted with antifarnesyl and anti-Flag antibodies. (C) Partitioning of 3xFlag AnkB in the detergent or aqueous phases of Triton X-114. Transfected cells were lysed with Triton X-114 and separated into detergent (D)-soluble and aqueous (Aq) phases. Samples were then analyzed by immunoblotting with anti-Flag antibodies. All experiments were performed three times, and representative examples are shown.

generated. The 3xFlag-tagged AnkB, AnkB^{169}C/A, or the control bacterial alkaline phosphatase (BAP) was ectopically expressed in HEK293 cells. Cell lysates were immunoprecipitated with anti-Flag antibody, and the immunoprecipitate was subjected to immunoblotting probed with anti-Flag followed by antifarnesyl antibody. The antifarnesyl antibody bound AnkB but not the AnkB^{169}C/A variant or the BAP negative control (Fig. 1 B). Examination by confocal microscopy showed that in contrast to AnkB, AnkB^{169}C/A was not localized to the plasma membrane but was distributed throughout the cytosol of HEK293 cells and *D. discoideum* (Fig. 1 A and Fig. S1). In addition, an intense colocalization of farnesylation with AnkB but not AnkB^{169}C/A or BAP was evident in HEK293 cells (Fig. 1 A).

Farnesylation of AnkB confers hydrophobicity

Because of hydrophobicity, farnesylated proteins partition into the detergent phase in Triton X-114 extractions (Bordier, 1981). Therefore, lysates of HEK293 cells ectopically expressing 3xFlag-tagged AnkB, AnkB^{169}C/A, or BAP control were solubilized with Triton X-114. The data showed that AnkB partitioned solely into the detergent phase, whereas AnkB^{169}C/A partitioned solely into the aqueous phase, similar to the cytosolic protein BAP (Fig. 1 C). Collectively, AnkB is farnesylated on the cysteine residue of the C-terminal CaaX motif, resulting in an increase in hydrophobicity and integration of AnkB into cellular membranes.

The CaaX motif of AnkB is sufficient for targeting a cytosolic protein to the plasma membrane

To determine whether the CaaX motif (CVLC) of AnkB was sufficient for targeting a cytosolic protein to the plasma membrane, we generated in-frame fusions of the last 12, 8, and 4 aa residues of AnkB to the C terminus of 3xFlag BAP (BAP^{12CaaX}, BAP^{8CaaX}, and BAP^{4CaaX}) and transfected HEK293. The data showed that although the native BAP was diffusely distributed throughout the cytosol, all of the three BAP^{12CaaX}, BAP^{8CaaX}, and BAP^{4CaaX} hybrid proteins localized primarily to the plasma membrane, similar to AnkB (Fig. 2 A). In Triton X-114, 52% of BAP^{4CaaX} partitioned into the detergent phase, whereas native BAP partitioned exclusively into the aqueous phase (Fig. 2 B).

To confirm the aforementioned data, lysates of transfected HEK293 cell expressing 3xFlag-tagged BAP or BAP^{4CaaX} were immunoprecipitated with anti-Flag antibody, and the immunoprecipitate was subjected to immunoblotting probed with anti-Flag followed by antifarnesyl antibody. The data showed that similar to AnkB, BAP^{4CaaX} but not BAP was recognized by the antifarnesyl antibody (Fig. 2 C). Therefore, the CaaX farnesylation motif of AnkB is sufficient for targeting a cytosolic protein to cellular membranes through farnesylation and subsequent increase in hydrophobicity of the modified protein.

Host cell farnesyltransferase is essential for targeting AnkB to host membranes

We determined the effect of chemical inhibition of host prenylation enzymes on targeting of AnkB to the plasma membrane. The HEK293 cells transfected with 3xFlag AnkB were pretreated with the farnesyltransferase or geranylgeranyltransferase inhibitors FTI-277 or GGTI-298, respectively (Lerner et al., 1995; McGuire et al., 1996), and analyzed by confocal microscopy. At all concentrations used in this study, neither FTI-277 nor GGTI-298 affected viability of HEK293 cells, as determined by trypan blue exclusion (unpublished data). The data showed that the farnesyltransferase inhibitor FTI-277 blocked membrane localization of AnkB at all concentrations above 10 nM up to 20 μM (Fig. 2 D). At a concentration of 10 nM, there was partial inhibition of membrane localization of AnkB, whereas at 5 nM, the inhibitor had no effect on membrane localization of AnkB (Fig. 2 D). In contrast, GGTI-298 blocked membrane localization of AnkB only at high concentrations of at least 10 μM (Fig. 2 D). To confirm these observations, we analyzed farnesylation of 3xFlag AnkB immunoprecipitated from transfected HEK293 cells treated with and without FTI-277 or GGTI-298, followed by immunoblotting with antifarnesyl antibody (Fig. 2 E). The data showed that treatment with 0.5–20 μM FTI-277 or 20 μM GGTI-298 blocked recognition of AnkB by the antifarnesyl antibody, compared with untreated cells (Fig. 2 E). In cells treated with 0.5 μM GGTI-298, AnkB was recognized by the antifarnesyl antibody, which is consistent with its membrane localization during treatment by that concentration (Fig. 2, D and E).

To confirm our chemical approach of inhibition of farnesyltransferase, we used farnesyltransferase-specific RNA interference (RNAi) to silence expression of the α subunit of farnesyltransferase (FT-α), the enzyme responsible for farnesylation of the cysteine residue within the CaaX motif (Reiss et al., 1990; Moores et al., 1991). Immunoblot analysis confirmed knockdown of FT-α expression by 48 h after treatment of HEK293 cells by RNAi without any detectable effect on viability (Fig. 2 G). Silencing FT-α in cells ectopically expressing 3xFlag-tagged AnkB and BAP^{4CaaX} resulted in a dramatic redistribution of AnkB and BAP^{4CaaX} from the plasma membrane into the cytosol (Fig. 2 F). In untreated cells, or in cells treated with a scrambled RNAi control, the AnkB and BAP^{4CaaX} proteins remained associated with the plasma membrane (Fig. 2 F). To confirm that silencing the expression of FT-α inhibited farnesylation, immunoprecipitation followed by immunoblotting were performed (Fig. 2 H). Silencing FT-α resulted in the inability of AnkB to bind the antifarnesyl antibody (Fig. 2 H). As expected, in untreated cells or cells treated with control RNAi, AnkB bound the antifarnesyl antibody (Fig. 2 H). Chemical inhibition or RNA-mediated knockdown of the host farnesylation machinery likely inhibited several trafficking pathways such as Rab localization to membranes. Collectively, the data show that the host farnesyltransferase is essential for farnesylation of AnkB on the C-terminal eukaryotic CaaX motif, resulting in its anchoring to the host membranes.

Farnesylation by macrophages and *D. discoideum* anchors AnkB to the cytosolic face of the LCV membrane

We used confocal microscopy to determine cellular location of AnkB at 2 h after infection of U937 macrophages and *D. discoideum* using rabbit anti-AnkB antiserum. Our data

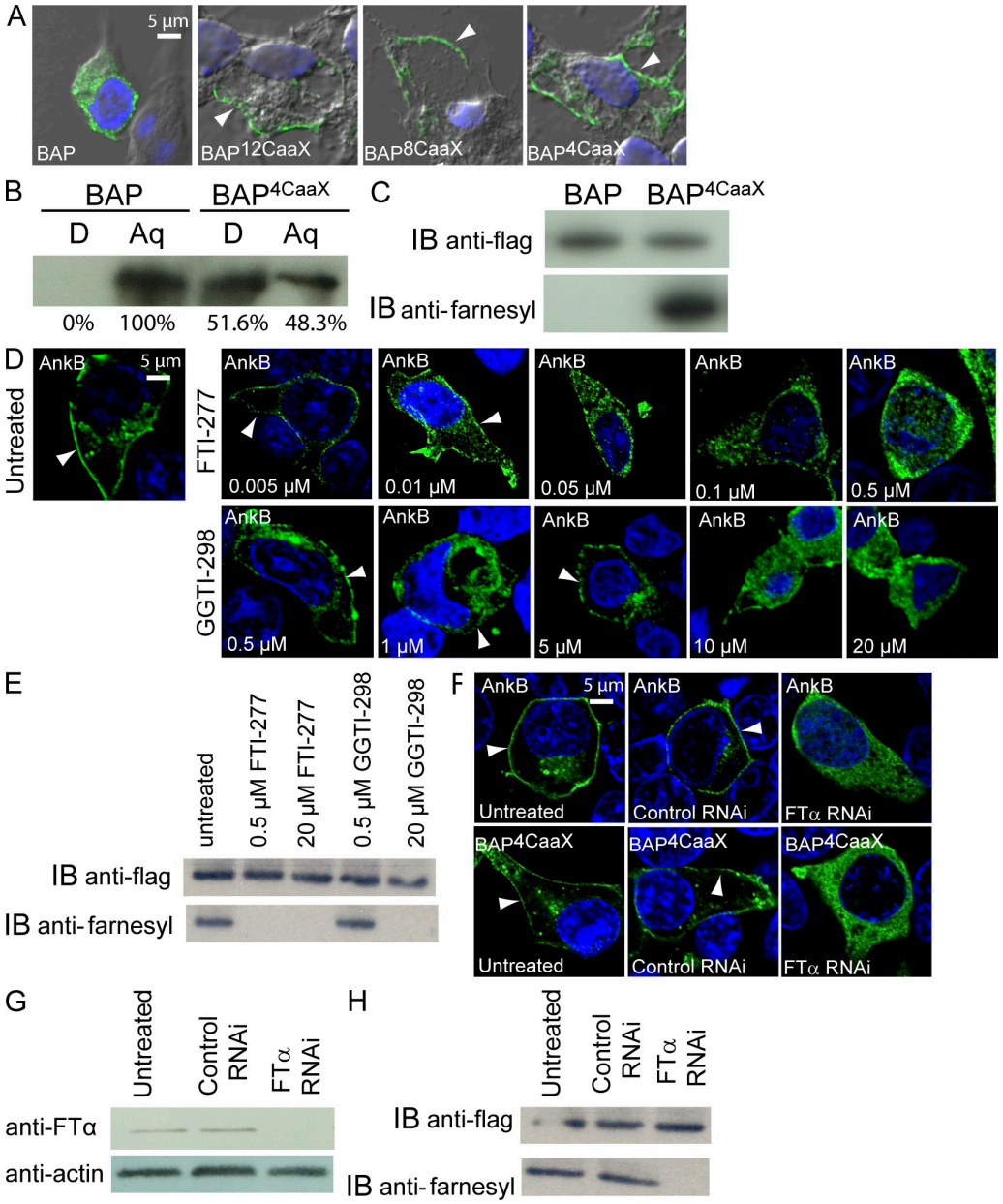

Figure 2. Host farnesyltransferase modifies ectopically expressed 3xFlag-tagged AnkB and BAP^{4CaaX} through the addition of a farnesyl moiety. (A) Representative confocal microscopy images of cells transfected with 3xFlag-tagged BAP, BAP^{12CaaX}, BAP^{8CaaX}, and BAP^{4CaaX}. The cells were labeled with anti-Flag antibody (green), whereas the nucleus is stained with DAPI (blue). Arrowheads indicate localization of the proteins to the plasma membrane. (B) Partitioning of 3xFlag-tagged BAP^{4CaaX} in Triton X-114 detergent (D) or aqueous (Aq) phases. Transfected cells were lysed with Triton X-114 and separated into detergent-soluble and aqueous phases. Samples were then analyzed by immunoblotting with anti-Flag antibodies. (C) 3xFlag-tagged BAP and BAP^{4CaaX} were immunoprecipitated from transfected HEK293 cells with anti-Flag resin and then analyzed by immunoblotting (IB) with antifarnesyl and anti-Flag antibodies. (D) Representative confocal images of HEK293 cells transfected with 3xFlag AnkB and treated with FTI-277 or GGTI-298 at concentrations of 0–20 µM. Anti-Flag labeling is represented in green, whereas the nucleus is stained blue (DAPI). Arrowheads indicate localization at the plasma membrane. All experiments were performed three times, and representative examples are shown. (E) Ectopically expressed 3xFlag AnkB in HEK293 cells treated with and without FTI-277 or GGTI-298 was immunoprecipitated with anti-Flag resin and then analyzed by immunoblotting with anti-Flag followed by antifarnesyl antibodies. (F) Knockdown expression of FT-α by RNAi blocks targeting of ectopically expressed 3xFlag-tagged AnkB and BAP^{4CaaX} to the plasma membrane. Representative confocal microscopy images of transfected untreated HEK293 cells or treated with scrambled control or FT-α–specific RNAi. Anti-Flag labeling is represented in green, whereas the nucleus is stained blue (DAPI). Arrowheads indicate localization of Flag-tagged proteins at the plasma membrane. (G) HEK293 cell lysates were immunoblotted with an anti–FT-α antibody followed by antiactin antibody. (H) Lysates of RNAi-treated HEK293 cells expressing 3xFlag AnkB were immunoprecipitated by anti-Flag antibodies, followed by immunoblotting with anti-Flag followed by antifarnesyl antibodies. All experiments were performed three times, and representative examples are shown.

showed localization of AnkB to the LCV harboring the WT strain in both macrophages and *D. discoideum* (Fig. 3 A and Fig. S2) but not the *ankB* mutant (Fig. 3 A). There was some background staining with anti-AnkB in the cytosol of noninfected and *ankB* mutant–infected U937 macrophages but none in *D. discoideum*. Therefore, AnkB seems to be exclusively localized to the LCV.

Next, we analyzed whether AnkB was located within the lumen of the LCV or on the cytosolic face of the LCV membrane. The LCVs were isolated at 2 h after infection of U937 macrophages and *D. discoideum* and probed with anti-AnkB antiserum before and after permeabilization of the LCV. The SidC effector that is known to localize to the cytosolic face of the LCV membrane was used as a positive control (Luo and Isberg, 2004). To ensure integrity of the isolated LCV preparations, we labeled nonpermeabilized LCVs with mouse anti–*L. pneumophila* monoclonal antibody, and after permeabilization with rabbit anti–*L. pneumophila* antiserum (Fig. 3 B). Our data showed that ∼95% of nonpermeabilized LCVs did not bind the mouse anti–*L. pneumophila* antibody, indicating that the isolation procedure did not disrupt the integrity of the LCV membrane (Fig. 3 B). When the LCVs were permeabilized before probing with both antibodies, both probes bound ∼95% of the bacteria within the LCVs (Fig. 3 C).

The data showed that before permeabilization, WT strain–containing purified LCVs from U937 macrophages and *D. discoideum* bound the anti-AnkB antibody, similar to the SidC positive control (Fig. 3 D and Fig. S2). Before permeabilization, the LCVs of the *ankB* mutant expressing AnkB^{169}C/A isolated from macrophages and *D. discoideum* did not bind the anti-AnkB antiserum (Fig. 3 D and Fig. S2) but did after permeabilization (Fig. 3 E and Fig. S2). We used the *dotA* mutant as a control because it expresses all effectors but is unable to translocate them because of the defect in the DotA structural component of the Dot/Icm translocation apparatus. As expected, nonpermeabilized LCVs harboring the translocation-defective *dotA* mutant (which expresses but does not translocate effectors) did not bind the anti-AnkB or anti-SidC antiserum (Fig. 3 D and Fig. S2). After permeabilization, the *dotA* mutant bound the anti-AnkB and anti-SidC antiserum within the LCVs as expected (Fig. 3 E). Both permeabilized and nonpermeabilized LCVs harboring the *ankB* mutant failed to bind the anti-AnkB antiserum (Fig. 3, D and E; and Fig. S2). Importantly, inhibition of farnesyltransferase blocked anchoring of AnkB to the cytosolic face of the LCV membrane (Fig. 3 G). This indicates that farnesylation of the conserved cysteine residue within the C-terminal CaaX motif is essential for anchoring AnkB to the cytosolic face of the LCV membrane within macrophages and *D. discoideum*.

To confirm farnesylation of AnkB localized to the LCV membrane, purified LCVs from infected U937 macrophages were subjected to immunoprecipitation using anti-AnkB antiserum, followed by immunoblotting probed with anti-AnkB followed by antifarnesyl antibody. The data showed that the AnkB derived from LCVs harboring WT bacteria was farnesylated (Fig. 3 F). In contrast, AnkB was not farnesylated in LCVs harboring *L. pneumophila* expressing AnkB^{169}C/A or the *dotA* translocation-defective mutant that is unable to translocate AnkB or other effectors (Fig. 3 F). Therefore, during infection, translocated AnkB localized to the LCV membrane is farnesylated, which is essential for its anchoring to the cytosolic face of the LCV membrane.

We investigated the potential of exploitation of the host farnesylation machinery by 20 bacterial pathogens and an endosymbiont that inject effectors into host cells by elaborate type III–VII secretion systems. Few housekeeping proteins contained the CaaX motif in most bacteria examined, and these were excluded from our analyses because they are unlikely to be effectors injected into the host cell. Interestingly, in silico genomic analyses have shown that all of these pathogens encode one or several C-terminal CaaX motif–containing proteins, compared with the genomes of nonpathogenic bacteria that have none, and some of these proteins are already documented effectors (Table S1), but the rest are of unknown function. In contrast, there were no CaaX motif–containing proteins encoded by the genomes of *Staphylococcus aureus*, *Streptococcus mutans*, *Corynebacterium diphtheriae*, or nonpathogenic *Escherichia coli* and *Bacillus subtilis*. Therefore, there is the potential of a widespread paradigm of exploitation of host cell farnesylation by bacterial pathogens that inject effectors into the host cell.

The CaaX motif of AnkB is indispensable for polyubiquitination of the LCV within macrophages and *D. discoideum*

To determine the functional role of farnesylation of AnkB during infection, we determined whether the C-terminal CaaX motif of AnkB was required for the docking of polyubiquitinated proteins to the LCV (Price et al., 2009). To test this, we infected U937 human macrophages and *D. discoideum* with the WT strain, the *ankB*-null mutant, or the *ankB* mutant complemented with the WT allele of *ankB* or the *ankB^{169}C/A* allele (Fig. 4, A and B). The infection was performed for 1 h at a multiplicity of infection (MOI) of 10, followed by 1-h treatment with gentamicin to kill extracellular bacteria. Essentially, similar results were found in human macrophages and *D. discoideum* (Fig. 4, A and B). After 2 h of infection, ∼90% of LCVs containing WT bacteria were decorated with polyubiquitinated proteins (Fig. 4 A), compared with only ∼20% of the LCVs harboring the *ankB* mutant (Fig. 4 A). The defect in polyubiquitination of the LCVs harboring the *ankB* mutant was completely restored by complementation with the WT *ankB* allele (Fig. 4, A and B). Importantly, LCVs harboring the *ankB* mutant complemented with the *ankB^{169}C/A* allele failed to be decorated with polyubiquitinated proteins, similar to the *ankB*-null mutant (Fig. 4, A and B). Therefore, farnesylation of AnkB is essential for its biological function as a platform for the docking of polyubiquitinated proteins to the LCV within human macrophages and *D. discoideum*.

The CaaX motif of AnkB is indispensable for intravacuolar proliferation within macrophages and *D. discoideum*

We determined the role of the CaaX motif in intravacuolar proliferation of the pathogen. Essentially, similar results were

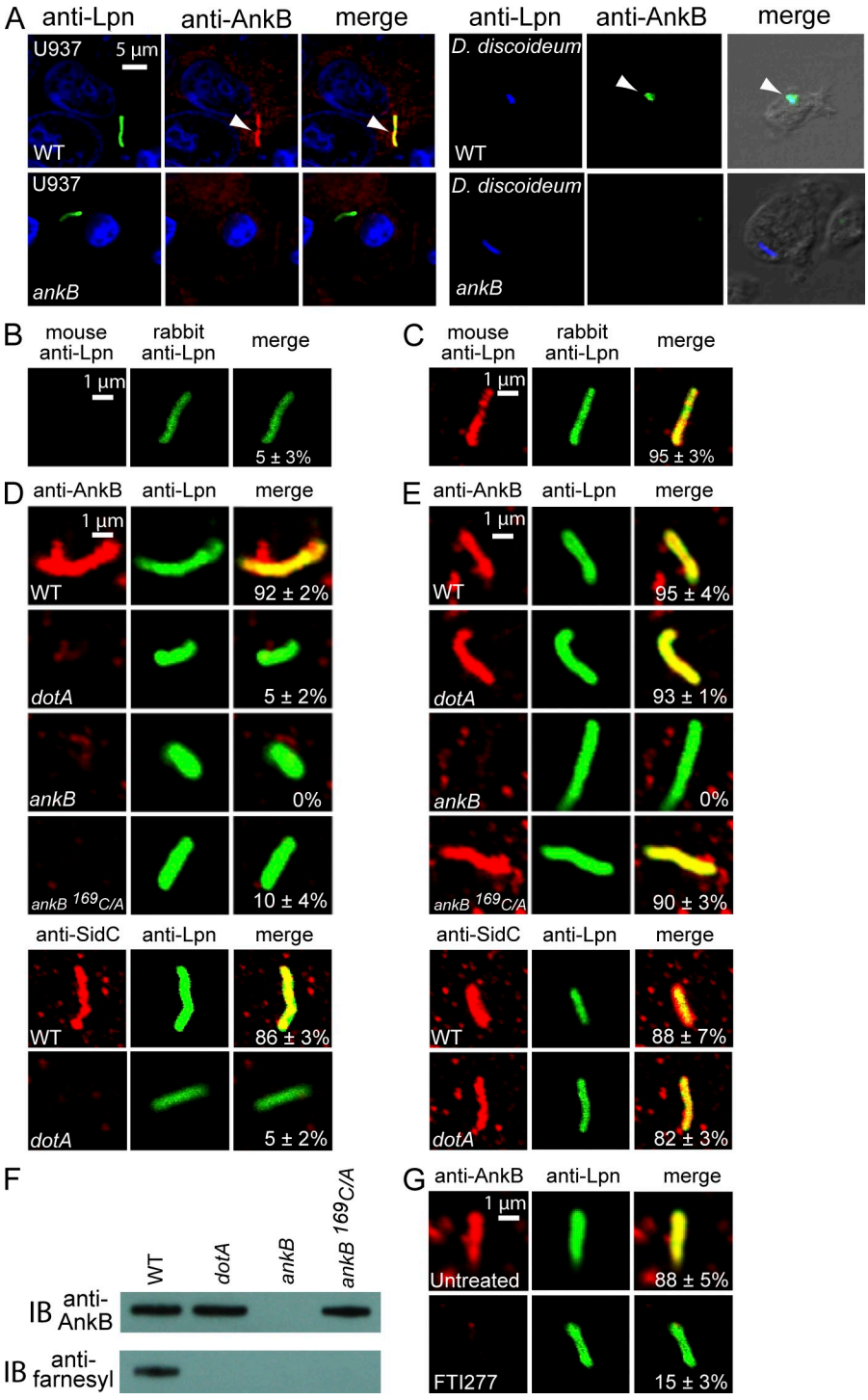

Figure 3. AnkB localizes to the LCV membrane through farnesylation of its CaaX motif. (A) The U937 cells and *D. discoideum* were infected and analyzed at 2 h by confocal microscopy using anti–*L. pneumophila* (Lpn) antibodies (green) and anti-AnkB antisera (red). Arrowheads indicate localization of AnkB with *L. pneumophila*. (B and C) Integrity of the membrane of purified LCVs from U937 cells was verified by labeling with mouse anti–*L. pneumophila* monoclonal antibody before permeabilization of the LCVs. After permeabilization, the LCVs were probed with rabbit anti–*L. pneumophila* antiserum to visualize the bacteria within the LCVs. (D and E) AnkB localizes to the cytosolic side of the LCV membrane. (D) The LCVs harboring the indicated strains were probed with anti-AnkB or anti-SidC antiserum before permeabilization (red) to determine whether the protein was localized to the cytosolic side of the LCV membrane. After permeabilization, the LCVs were probed with mouse anti–*L. pneumophila* monoclonal antibodies (green) to visualize the bacteria within the LCV. Quantitation is shown in the merged panels, where the numbers represent the percentage plus standard deviation of LCVs that bound anti-AnkB or anti-SidC antiserum before permeabilization. Analyses were based on the examination of 100 LCVs from triplicate samples. (E) The LCVs were permeabilized and then labeled with anti-AnkB or anti-SidC antiserum and anti–*L. pneumophila* monoclonal antibody, and quantitation of the LCVs that bound both antibodies is shown in the merged images and is based on analyses of 100 LCVs. (F) Farnesylation of AnkB anchors it to the LCV membrane. The AnkB proteins were immunoprecipitated using anti-AnkB antisera and then analyzed by immunoblotting (IB) with anti-AnkB followed by antifarnesyl antiserum. (G) The FTI-277 blocks localization of AnkB to the cytosolic side of the LCV membrane. The LCVs were isolated from untreated or 0.5 µM FTI-277–treated U937 cells at 1 h after infection and labeled with anti-AnkB antiserum before permeabilization (red). After permeabilization, the LCVs were labeled with anti–*L. pneumophila* monoclonal antibody (green) and analyzed by confocal microscopy. Quantification is shown in the merged panels, where the numbers represent the percentage plus standard deviation of LCVs that bound anti-AnkB before permeabilization. Analyses were based on examination of 100 LCVs from triplicate samples. All experiments were performed in triplicate, and representative examples are shown. All the results in this figure are representative of three independent experiments.

found in U937 macrophages and *D. discoideum* (Fig. 4, C and D). The data showed that the WT strain proliferated robustly within macrophages and *D. discoideum*, whereas the *ankB* mutant was defective in intracellular proliferation (Fig. 4 C). Complementation of the *ankB* mutant with the WT *ankB* allele restored replication, similar to the WT strain (Fig. 4 C). In contrast, complementation of the *ankB* mutant with the *ankB*^{169}*C/A* allele failed to restore intracellular replication to the *ankB* mutant within macrophages and *D. discoideum*. Therefore, the C-terminal CaaX motif of AnkB is essential

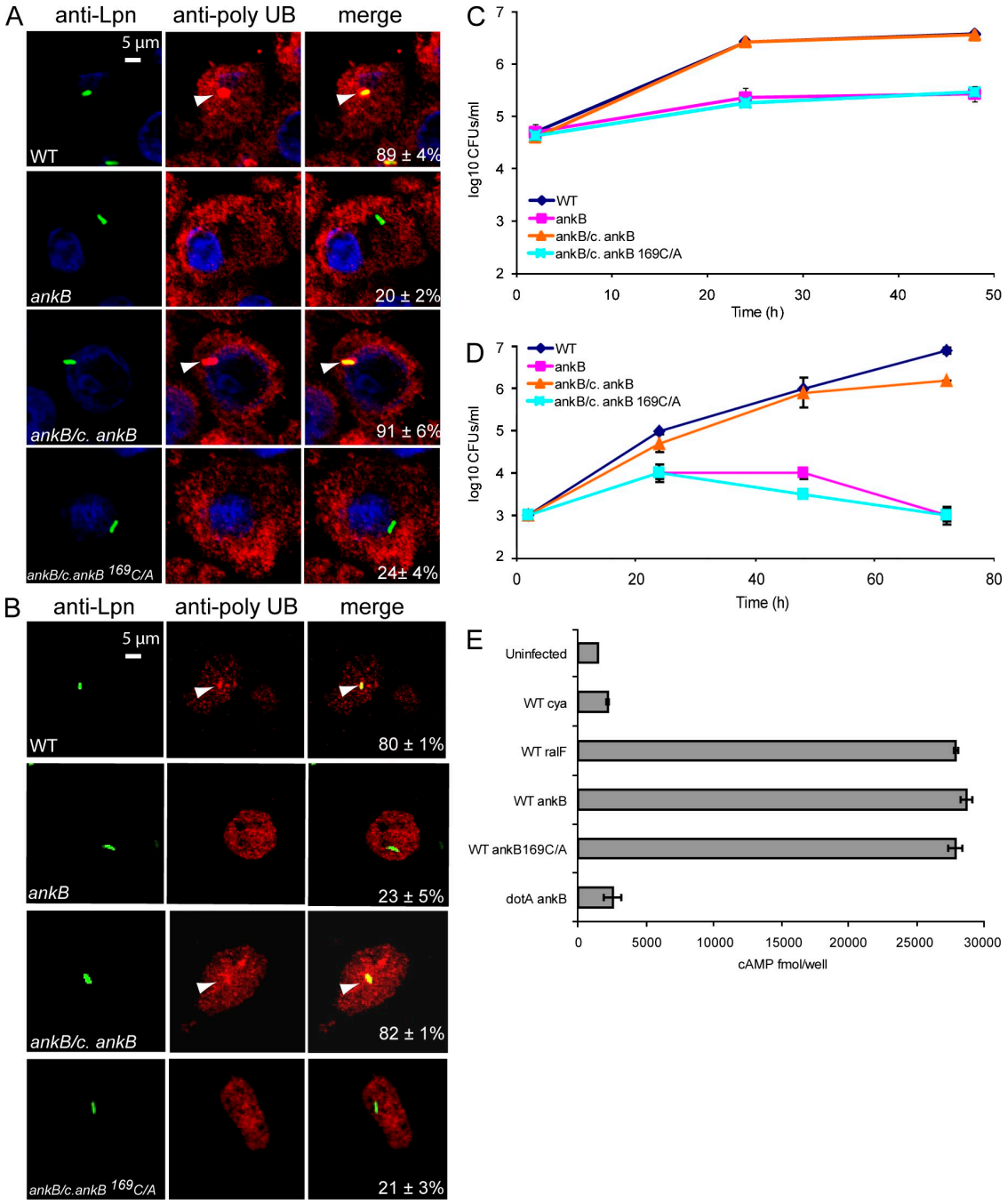

Figure 4. The CaaX motif of AnkB is essential for polyubiquitination of the LCV and for intracellular bacterial replication. (A and B) Representative confocal microscopy images of U937 cells (A) and *D. discoideum* cells (B) infected with *L. pneumophila* and examined at 2 h after infection for recruitment of polyubiquitinated proteins to the LCV. The U937 and *D. discoideum* cells were infected with the WT strain, the *ankB* mutant, and the *ankB* mutant complemented with the WT allele of *ankB* (*ankB*/c.*ankB*) or *ankB*^{169}*C/A* (*ankB*/c.*ankB*^{169}*C/A*) allele. Bacteria are labeled with anti-*L. pneumophila* (Lpn) antibody (green), polyubiquitinated (poly UB) proteins are labeled red, and the nucleus is stained blue (DAPI). Arrowheads indicate heavy colocalization of polyubiquitin with the LCVs. Numbers in the merged panels are quantitation of the percentage of LCVs positive for recruitment of polyubiquitinated proteins, based on the examination of 100 LCVs in triplicate samples. (C and D) Intracellular growth kinetics of *L. pneumophila* strains in U937 cells (C) or *D. discoideum* (D) infected with the WT strain, the *ankB* mutant, and the *ankB* mutant complemented with the WT copy of the *ankB* or the *ankB*^{169}*C/A* allele. (E) Translocation of AnkB into U937 cells was determined at 1 h after infection. Strains harbored either empty vector (pCya) or Cya hybrids of RalF, AnkB, or AnkB^{169}C/A. The translocation-defective *dotA* mutant harboring AnkB-Cya was used as a negative control. All experiments were performed three times, and representative examples are shown. (C–E) The data are the mean of triplicate samples, and the error bars are the standard deviations.

for intravacuolar proliferation of *L. pneumophila* within human macrophages and *D. discoideum*.

Translocation of AnkB^{169}C/A into the host cell

To examine whether substitution of cysteine for alanine in the C-terminal CaaX motif affected translocation of AnkB^{169}C/A by the Dot/Icm type IV translocation system, we used the calmodulin-dependent adenylate cyclase reporter fusion assay using ELISA (Al-Khodor et al., 2008; Sory and Cornelis, 1994). The U937 cells were infected for 1 h with the WT strain harboring the vector alone, *ralF*-CyaA as a control, *ankB*-CyaA, or *ankB^{169}C/A*-CyaA. The translocation-defective *dotA* mutant harboring *ankB*-CyaA was used as a negative control. The data showed that AnkB^{169}C/A was translocated into the host cell cytosol similar to native AnkB and the RalF effector control (Fig. 4 E).

Host farnesyltransferase is essential for the docking of polyubiquitinated proteins to the LCV within macrophages and *D. discoideum*

To determine whether host-mediated farnesylation of AnkB was important for polyubiquitination of the LCV, U937 cells

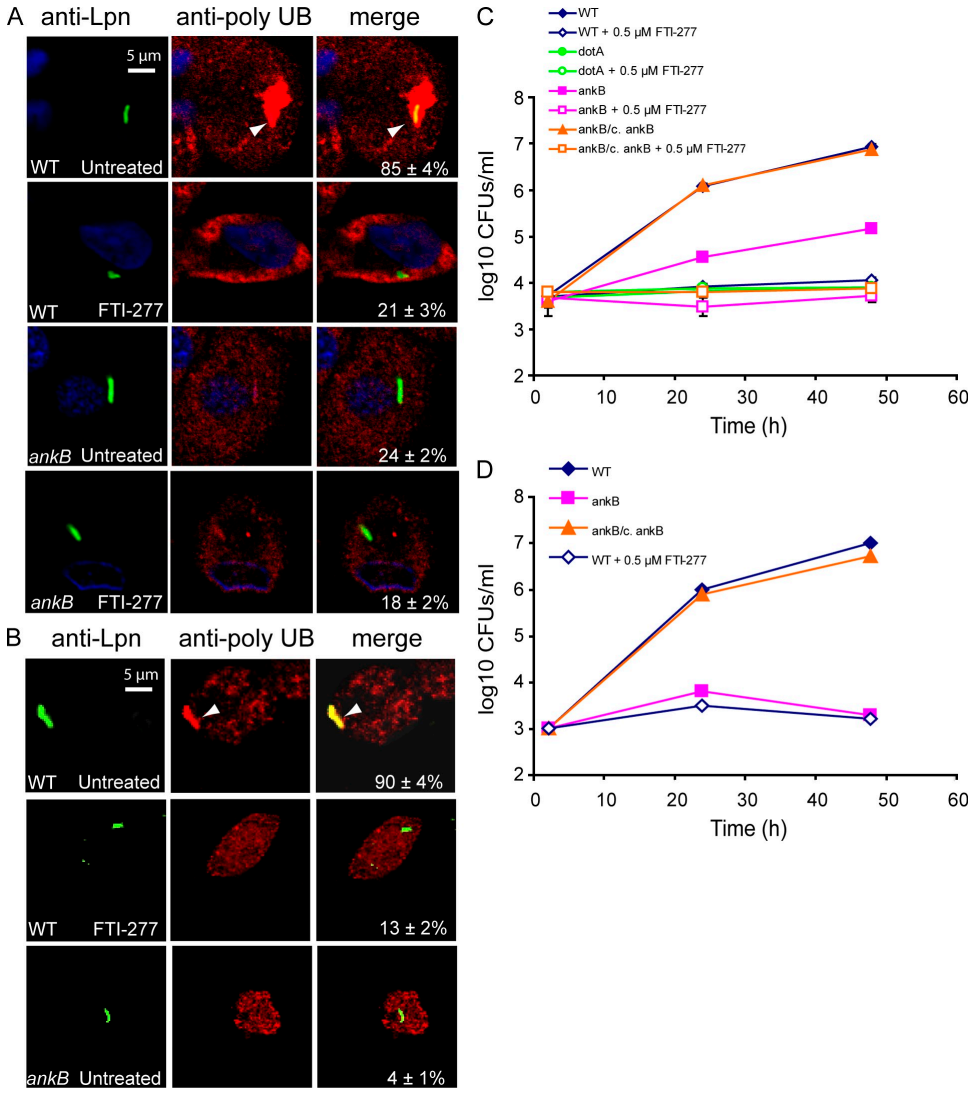

Figure 5. Chemical inhibition of host FT-α blocks recruitment of polyubiquitinated proteins to the LCV and abolishes intravacuolar bacterial replication. (A and B) Representative confocal microscopy images of cells untreated or treated with 0.5 µM FTI-277 for U937 cells (A) and *D. discoideum* (B). The host cells were infected with the WT strain or the *ankB* mutant, and recruitment of polyubiquitinated (poly UB) proteins to the LCV was examined at 2 h after infection. Bacteria are labeled by anti–*L. pneumophila* (Lpn) antibody (green), polyubiquitin is labeled red, and the nucleus is stained blue (DAPI). Arrowheads indicate heavy colocalization of polyubiquitinated proteins with the LCVs. Numbers in the merged panels are quantitation of the percentage of LCVs that colocalized with polyubiquitinated proteins at 2 h after infection, based on the examination of 100 LCVs from triplicate samples. (C and D) Intracellular growth kinetics of *L. pneumophila* strains in cells untreated or treated with and without 0.5 µM FTI-277 for U937 cells (C) or *D. discoideum* (D). The cells were infected with the WT strain, the *ankB* mutant, and the *ankB* mutant complemented with the WT copy of the *ankB* or the *ankB^{169}C/A* allele. The results are representative of three independent experiments performed in triplicate, and error bars represent standard deviation.

and *D. discoideum* were pretreated with 0.5 μM of the farnesyltransferase inhibitor FTI-277 (Fig. 5, A and B). At the concentrations used in our experiments, the FTI-277 inhibitor had no detectable effect on bacterial proliferation in vitro (unpublished data). Essentially, similar results were found in U937 cells (Fig. 5 A) and *D. discoideum* (Fig. 5 B). After 2- and 12-h infection of untreated cells with the WT bacteria, most LCVs were decorated with polyubiquitinated proteins (Fig. 5, A and B). However, in cells treated with FTI-277, most LCVs containing WT bacteria were not decorated with polyubiquitinated proteins at 2 and 12 h, similar to the *ankB*-null mutant in untreated cells (Fig. 5, A and B). Therefore, chemical inhibition of farnesyltransferase in macrophages and in *D. discoideum* results in a loss of biological function of AnkB.

To confirm the chemical approach, we used a genetic approach to knockdown expression of FT-α by RNAi (Fig. 2 G). The RNAi-treated HEK293 cells were infected after 48 h of RNAi treatment and examined by microscopic single cell analyses for decoration of the LCV by polyubiquitinated proteins. The data showed that in untreated cells and in cells treated with a scrambled RNAi control, most LCVs of the WT strain were decorated with polyubiquitinated proteins at 2 and 12 h after infection (Fig. 6 A). However, in cells treated with FT-α–specific RNAi, most LCVs were not decorated with polyubiquitinated proteins at 2 and 12 h after infection, similar to the *ankB*-null mutant (Fig. 6 A and not depicted). Collectively, we conclude that farnesylation of AnkB by the host farnesyltransferase is indispensable for the biological function of the F-box–containing AnkB effector.

Host farnesyltransferase is essential for intracellular replication of *L. pneumophila* and other *Legionella* species

To determine whether host-mediated farnesylation of AnkB was required for intracellular replication, U937 cells

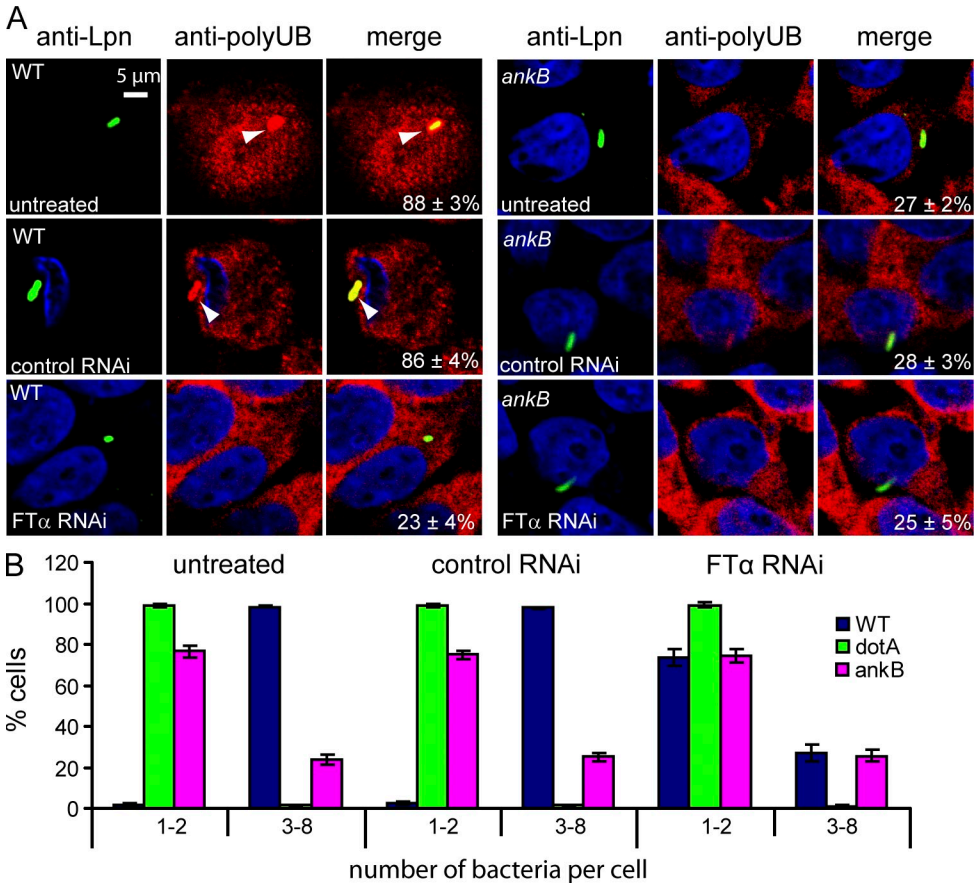

Figure 6. Knockdown of expression of host FT-α by RNAi blocks recruitment of polyubiquitinated proteins to the LCV and abolishes intravacuolar bacterial replication. (A) Representative confocal images of untreated HEK293 cells or cells treated with FT-α–specific or scrambled RNAi control. The cells were infected with the WT strain or the *ankB* mutant bacteria, and recruitment of polyubiquitinated proteins to the LCV was examined at 2 h after infection. Bacteria are labeled with anti–*L. pneumophila* (Lpn) antibody (green), polyubiquitinated (polyUB) proteins are labeled red, and the nucleus is stained blue (DAPI). Arrowheads indicate heavy colocalization of the LCVs with polyubiquitinated proteins. Numbers in the merged panels are the percentage of LCVs positive for polyubiquitin plus standard deviation, based on the examination of 100 LCVs from triplicate samples. (B) Quantitation by single cell analysis of bacterial replicative phagosomes in HEK293 cells at 12 h after infection based on the analyses of 100 infected cells by confocal microscopy and presented as the number of bacteria/cell and the percentage of cells harboring a certain number of bacteria. The *dotA* mutant was used as a negative control. Infected cells from multiple coverslips were examined in each experiment. The results are representative of three independent experiments performed in triplicate, and error bars represent standard deviation.

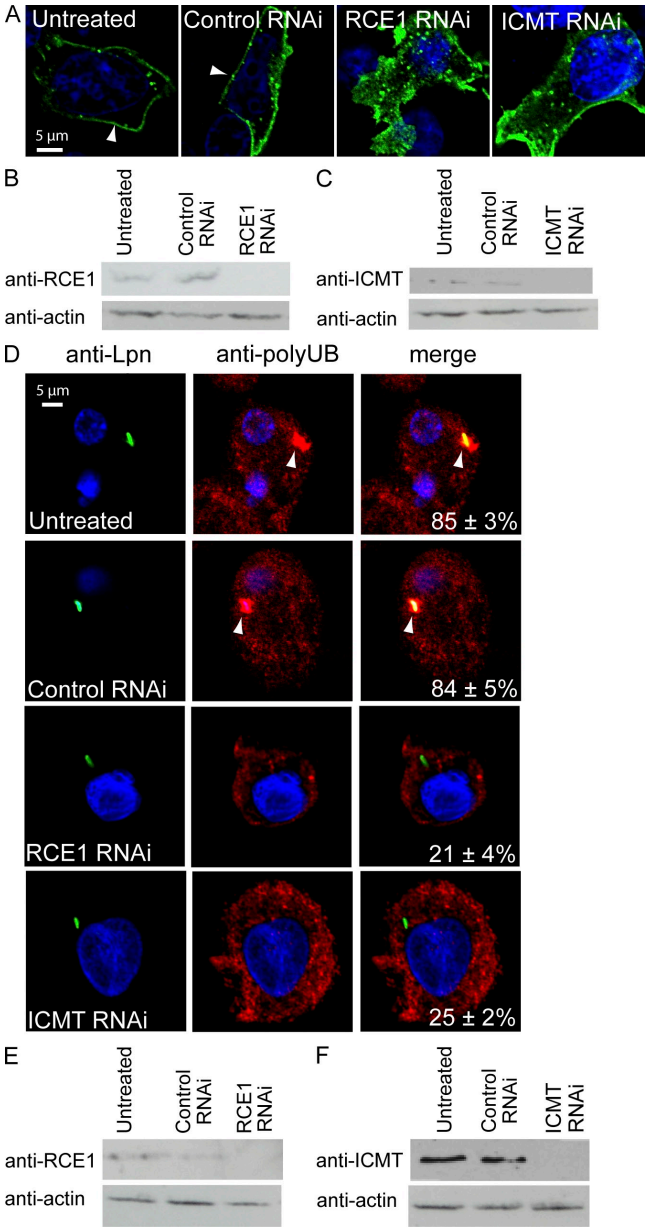

Figure 7. RNAi knockdown of ICMT and RCE-1 blocks targeting of AnkB to membranes and inhibits the biological function of the F-box protein in decorating the LCV by polyubiquitinated proteins. (A) Representative confocal microscopy images of untreated HEK293 cells or RNAi control–treated or ICMT- or RCE-1–specific RNAi–treated cells transfected with 3xFlag-tagged AnkB. The cells were labeled with anti-Flag antibody (green), whereas the nucleus is stained with DAPI (blue). Arrowheads indicate localization of the proteins to the plasma membrane. (B and C) RNAi-mediated knockdown expression of RCE-1 and ICMT, respectively. (D) Representative confocal images of untreated U937 cells or cells treated with the indicated RNAi. The cells were infected with the WT strain, and recruitment of polyubiquitinated proteins to the LCV was examined at 2 h after infection. Bacteria are labeled with anti–*L. pneumophila* (Lpn) antibody (green), polyubiquitinated (polyUB) proteins are labeled red, and the nucleus is stained blue (DAPI). Arrowheads indicate heavy colocalization of the LCVs with polyubiquitinated proteins. Numbers in the merged panels are the percentage of LCVs positive for polyubiquitin plus standard deviation, based on the examination of 100 LCVs from triplicate samples. (E and F) RNAi-mediated knockdown expression of RCE-1 and ICMT, respectively. All the results in this figure are representative of three independent experiments.

and *D. discoideum* were pretreated with 0.5 µM of the farnesyltransferase inhibitor FTI-277, and the intracellular growth kinetics were measured. The data showed that the inhibitor suppressed intracellular proliferation within human cells and *D. discoideum* (Fig. 5, C and D). These results were further confirmed by single cell analysis using confocal microscopy (Fig. S3).

To determine whether exploitation of the host farnesylation was required for intracellular proliferation of other *Legionella* species, we determined the effect of inhibition of the host farnesylation by FTI-277 on intracellular replication of *Legionella micdadei*, *Legionella dumoffii*, and two strains of *Legionella longbeachae*. Confocal microscopy was used to determine the formation of a replicative vacuole at 12 h after infection at a low MOI. Although at 2 h there was a single bacterium in most infected cells, the formation of a replicative vacuole at 12 h was evident for all the strains in untreated cells. However, inhibition of the host farnesylation machinery blocked intracellular proliferation for all the strains (Fig. S4). Thus, exploitation of the host farnesylation is exhibited by other *Legionella* species and is likely so for many other intracellular pathogens that express CaaX motif–containing proteins (Table S1).

To confirm the chemical approach, we silenced the expression of FT-α by RNAi in HEK293 cells before infection by *L. pneumophila*. Single cell analyses by confocal microscopy showed that in FT-α RNAi–treated cells, bacterial replication was severely inhibited when examined at 12 h after infection because most cells harbored a single organism (Fig. 6 B). This was in stark contrast to untreated cells or cells treated with scrambled RNAi control, in which most cells harbored approximately eight WT bacteria (Fig. 6 B). Collectively, these data confirm that host farnesyltransferase is an essential enzyme for the biological function of AnkB.

To determine whether inhibition of farnesyltransferase altered trafficking of the LCV, we used confocal laser-scanning microscopy to assess colocalization of the LCV with the late endosomal/lysosomal marker LAMP-2 and the luminal lysosomal enzyme cathepsin D at 2 h after infection of U937 cells, using formalin-killed bacteria as a positive control. The data showed that inhibition of host farnesyltransferase did not alter trafficking of the LCV (Fig. S5).

The RCE-1 and ICMT host enzymes are essential for the biological function of AnkB

Our aforementioned data have shown the PFT was essential for the biological function of AnkB. To determine whether RCE-1 and ICMT were also required for the biological function of AnkB, expression of either of the two proteins was knocked down by specific RNAi in HEK293 cells to determine the effect on localization during ectopic expression (Fig. 7, B and C).

Cells transfected with Flag-tagged AnkB showed that RCE-1 was essential for targeting AnkB to the plasma membrane, whereas ICMT had a partial role because reduced membrane localization was evident in the knocked down cells (Fig. 7 A).

During infection of U937 macrophages by the WT strain, knockdown expression of RCE-1 or ICMT (Fig. 7, E and F) caused a complete inhibition of the biological function of AnkB as a platform for the docking of polyubiquitinated proteins to the LCV, whereas the RNAi control had no effect (Fig. 7 D). Collectively, the host three enzymes FT-α, RCE-1, and ICMT are essential for the biological function of AnkB.

Dot/Icm-dependent recruitment of FT-α, RCE-1, and ICMT with the LCV

The LCV membrane is derived from the ER, which is the site for cleavage of the -aaX tripeptide and methylation of the farnesylated cysteine of the CaaX motif. This led us to examine whether host FT-α, RCE-1, and ICMT were recruited to the LCV within macrophages using confocal microscopy (Fig. 8, A–C). Strikingly, at 2 h after infection, 75–85% of the LCVs harboring WT bacteria within macrophages colocalized with the three host enzymes (Fig. 8, A–C), compared with ∼20% of the LCVs harboring the *dotA* translocation-defective mutant. This indicated that recruitment of the host FT-α, RCE-1, and ICMT required a functional Dot/Icm type IV translocation apparatus (Fig. 8, A–C). Interestingly, the *ankB* mutant exhibited a slight but significant (Student's *t* test, $P < 0.001$) reduction in colocalization with host FT-α relative to WT bacteria, which was reversed by complementation of the *ankB* mutant with the WT *ankB* allele (Fig. 8, A–C). In contrast, complementation of the *ankB* mutant with the *ankB*^{169}*C/A* allele did not restore colocalization of the LCV with host FT-α, compared with the *ankB* mutant complemented with the WT *ankB* allele (Fig. 8, A–C). Colocalization of the LCVs with the host FT-α was further confirmed using purified LCVs from infected macrophages at 2 h after infection (Fig. S6). This indicates that other Dot/Icm-translocated effectors play a crucial role in recruiting the host FT-α, RCE-1, and ICMT to the LCV.

Farnesylation of AnkB is essential for intrapulmonary proliferation in the mouse model

To determine whether farnesylation of AnkB was required in vivo for intrapulmonary proliferation of *L. pneumophila*, we infected A/J mice with 10^6 CFUs of *L. pneumophila* WT strain,

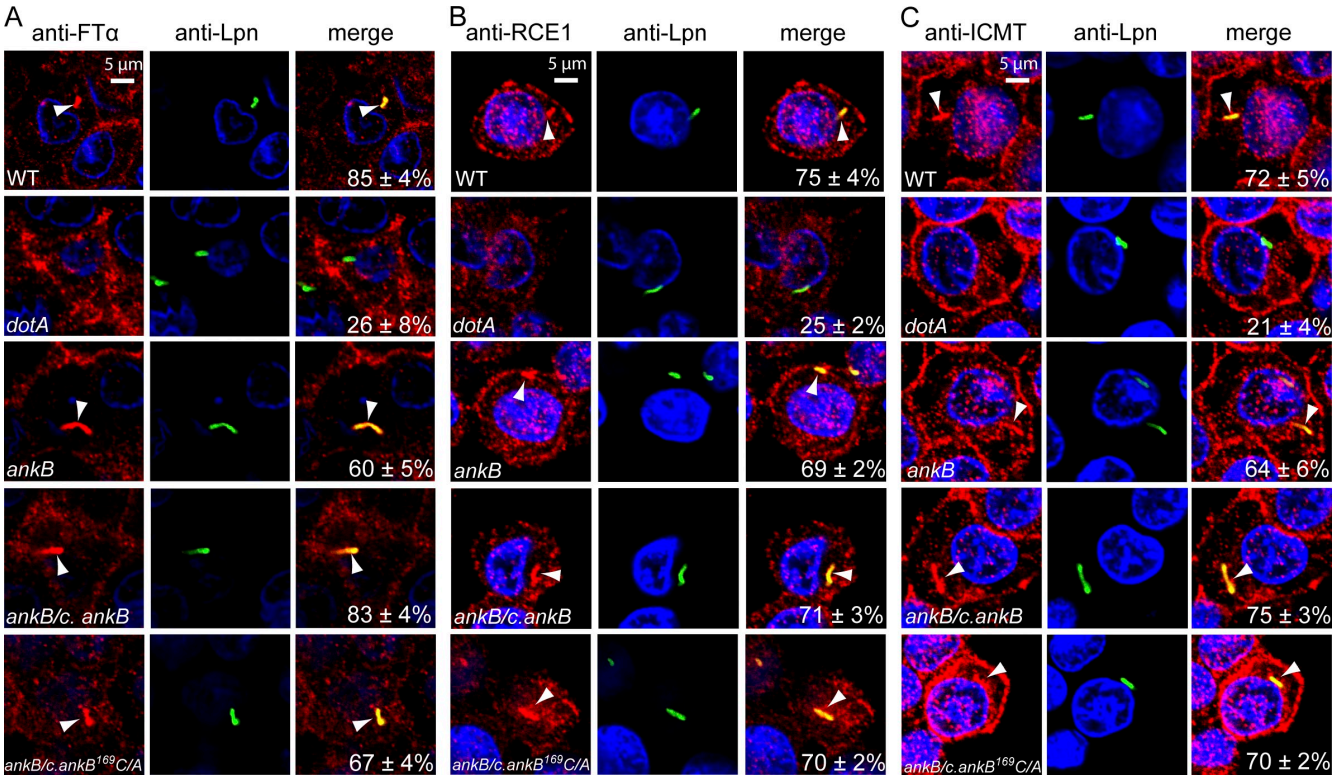

Figure 8. Dot/Icm-dependent colocalization of the LCV with the three enzymes FT-α, RCE-1, and ICMT. (A–C) The U937 cells were infected with WT, *dotA*, *ankB*, *ankB*|c.*ankB*, and *ankB*|c.*ankB*^{169}*C/A* bacteria. At 2 h after infection, the cells were labeled with anti–*L. pneumophila* (Lpn) antibodies (green) and anti–FT-α (A), anti–RCE-1 (B), or anti-ICMT (C) antibodies (red). Nuclei were stained with DAPI (blue). The cells were analyzed by confocal microscopy. Arrowheads indicate colocalization of the respective marker with the LCVs. Quantification is shown in the merged images and represents a total percentage of LCVs colocalized with the maker plus standard deviation, based on the examination of 100 cells from triplicate samples. All experiments were performed three times, and representative examples are shown.

the *ankB* mutant, the *ankB* mutant complemented with the WT *ankB* allele, or the *ankB*^{169}*C/A* allele. There was robust intrapulmonary proliferation by the WT strain and the *ankB* mutant complemented with the WT *ankB* allele (Fig. 9). In contrast, there was no detectable intrapulmonary proliferation for the *ankB* mutant complemented with *ankB*^{169}*C/A* allele (Student's *t* test, $P < 0.001$), which was indistinguishable from the *ankB*-null mutant (Fig. 9). We conclude that farnesylation of AnkB is essential for its function in vivo in the mouse model of Legionnaires' disease, which is consistent with its indispensable role in intracellular proliferation in vitro.

DISCUSSION

Although numerous bacterial effectors of various intravacuolar pathogens are localized to the pathogen-containing vacuolar membrane, the mechanisms are not well known. Our data provide a potentially new paradigm for anchoring microbial effectors to the pathogen-containing vacuolar membrane. We provide several lines of evidence from the host and from the microbe sides to confirm that the conserved cysteine residue in the CaaX motif of AnkB is farnesylated by the host farnesyltransferase, leading to anchoring of AnkB to the LCV membranes within evolutionarily distant host cells.

We have recently provided the first demonstration of specific and mechanistic exploitation of conserved eukaryotic processes in amoeba and macrophages by *L. pneumophila* through the Dot/Icm-translocated AnkB effector, which exhibits molecular and functional mimicry of eukaryotic F-box proteins (Price et al., 2009). Anchored to the cytosolic face of the LCV membrane by host-mediated farnesylation, AnkB functions as a platform for the docking of polyubiquitinated proteins to the LCV membrane (Price et al., 2009). Therefore, exploitation of host farnesylation is the second evolutionarily conserved eukaryotic machinery exploited by the same effector to enable intravacuolar proliferation of *L. pneumophila* within evolutionarily distant hosts (Molmeret et al., 2005; Franco et al., 2009). Anchoring of the bacterial F-box effector to the cytosolic face of the pathogen-containing vacuolar membrane is novel among the large family of mammalian F-box proteins that are not anchored to membranes by farnesylation.

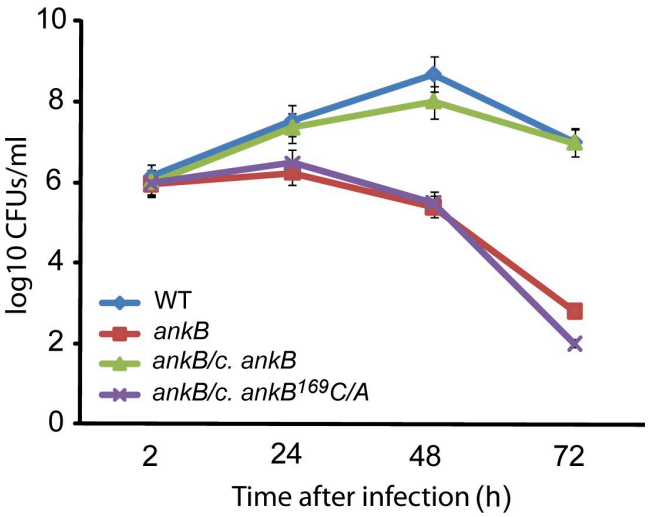

Figure 9. *L. pneumophila* expressing the *ankB*^{169}*C/A* allele is defective in intrapulmonary proliferation in the A/J mice model of Legionnaires' disease. Three A/J mice for each time point were infected with 10^6 CFUs of *L. pneumophila* WT strain, the *ankB* mutant, or the *ankB* mutant complemented with either the WT *ankB* allele (*ankB/c.ankB*) or with the *ankB*^{169}*C/A* allele (*ankB/c.ankB*^{169}*C/A*). At each time point, three mice were sacrificed, lungs were obtained and homogenized, and dilutions were plated on agar plated for CFU enumeration. The results are the mean of three mice/time point. These results are representative of two independent experiments. Error bars indicate standard deviation.

The AnkB F-box effector is the only microbial translocated effector known to be modified by the host cell PFT machinery, which is essential for biological function in intravacuolar proliferation (Price et al., 2009), which is novel. The SifA effector of *Salmonella typhimurium* is translocated by the type III secretion system and is localized to the *Salmonella*-induced filaments that connect *Salmonella*-containing vacuoles, but its biological function is not known (Boucrot et al., 2003; Reinicke et al., 2005). When ectopically expressed in transformed epithelial cells, SifA is prenylated by PGGT and is targeted to membranes (Boucrot et al., 2003; Reinicke et al., 2005). However, prenylation of SifA by PGGT is dispensable for its biological function because a *sifA* substitution mutant blocked from prenylation is fully competent in intracellular proliferation and virulence in the mouse model (Reinicke et al., 2005). In contrast, PFT-mediated farnesylation of AnkB is essential for its biological function, which is novel. Our data show the first example for the role of host farnesylation of the bacterial effector in proliferation of the pathogen in vivo in the mouse model of the disease. This clearly shows a remarkable and intimate microbe–host interaction that requires modification of the microbial effector by the host enzymes to manifest disease.

Although farnesyltransferase is cytosolic, it is recruited to the LCV in a Dot/Icm-dependent manner (Segal et al., 1998; Vogel et al., 1998), which may enable local farnesylation of AnkB at the LCV membrane that is ER derived (Tilney et al., 2001; Kagan and Roy, 2002). Farnesylated proteins often undergo further posttranslational modifications at the ER membrane RCE-1 and ICMT (Wright and Philips, 2006) to cleave the terminal -aaX tripeptide and methylate the terminal farnesylated cysteine residue, respectively. Importantly, the three host enzymes are essential for the biological function of AnkB. Because all three host enzymes are recruited to the ER-derived LCV and AnkB is only detectable in the LCV and not in the cytosol, we propose that farnesylation and posttranslational processing of the C terminus of the farnesylated AnkB effector occur locally at the ER-derived LCV membrane. However, it is also possible that undetectable amounts of AnkB traffic to the cytosol before anchoring to the LCV membrane. Our data provide the first example of an intravacuolar pathogen that hijacks the farnesylation machinery of the host through bacterial-mediated recruitment of the three host enzymes to the pathogen-containing vacuole. Because recruitment of the three host enzymes to the

LCV is Dot/Icm dependent, it is likely that other effectors are involved in recruitment of at least PFT, whereas ICMT and RCE-1 can simply be ER-resident proteins and are components of the ER-derived LCV membrane. Our data show that exploitation of host farnesylation is essential for intracellular proliferation of many other *Legionella* species. It is likely that other intravacuolar pathogens that reside within non-ER or ER-derived vacuoles such as *Mycobacterium tuberculosis*, *Salmonella enterica*, *Anaplasma marginale*, *Bartonella henselae*, and *Brucella abortus* may exploit the host farnesylation machinery similar to *L. pneumophila* to allow farnesylation and anchoring of microbial effectors to the pathogen-containing vacuolar membrane.

MATERIALS AND METHODS

Bacterial strains, cell cultures, and infections. *L. pneumophila* strain AA100/130b (BAA-74; American Type Culture Collection) and the isogenic mutants *dotA*, *ankB*, and complemented *ankB* mutants were grown as described previously (Al-Khodor et al., 2008). The *L. longbeachae* strains (Asare and Abu Kwaik, 2007; Asare et al., 2007) and *L. micdadei* and *L. dumoffii* strains (Alli et al., 2003) have been previously described. *E. coli* strain DH5-α was used for cloning purposes. Maintenance of U937 and HEK293 cells was performed as previously described (Price et al., 2009). The *D. discoideum* WT strain AX2 was grown axenically at 24°C in HL5 medium supplemented with 0.6% penicillin-streptomycin and 20 μg/ml G418 as needed at 22°C, as we described previously (Price et al., 2009). Infection and intracellular proliferation experiments were performed as we described previously (Price et al., 2009). In brief, macrophages were infected at a MOI of 10 for 1 h, followed by treatment with 50 μg/ml gentamicin for 1 h to kill extracellular bacteria. At several time points, the cells were lysed, and dilutions were plated on agar plates. Isolation of the LCVs was performed as we described previously (Price et al., 2009). Measurement of cAMP in cell lysates for adenylate cyclase fusion assays was performed using the Direct Cyclic AMP Enzyme Immunoassay kit (Enzo Life Sciences, Inc.), as we described previously (Al-Khodor et al., 2008).

Transfections and inhibitors. Cloning of the 3xFlag-tagged *ankB*^{169}*C/A* and BAP alleles was performed as described previously (Price et al., 2009), using specific primers (Table S2). HEK293 cells were transfected using Fugene HD reagent (Roche), as we described previously (Price et al., 2009). The various *ankB* mutant alleles were used as templates to create 3xFlag fusions in plasmid p3xFlag pDM320 for expression in *D. discoideum* using specific primers (Table S2). *D. discoideum* were transformed by electroporation according to standard protocols (Pang et al., 1999), and the cells were grown in HL5 containing 20 μg/ml G418.

The inhibitors FTI-277 and GGTI-298 (EMD) were resuspended in DMSO + 0.4 mM dithiothreitol and used immediately and were maintained in the growth media throughout the experiment. Silencing of FT-α, ICMT, and RCE-1 by RNAi in HEK293 or U937 cells (Santa Cruz Biotechnology, Inc.) was performed as we described previously (Price et al., 2009).

Triton X-114 partitioning, immunoprecipitation, and immunoblotting. Cells were lysed in M-PER reagent (Thermo Fisher Scientific) containing a protease inhibitor cocktail (Complete Mini EDTA-free; Roche). Flag-tagged proteins were purified using anti-Flag M2 resin (Sigma-Aldrich) and subjected to immunoblot analysis using an antifarnesyl antibody (1:200 dilution; Abcam), anti-Flag antibody (1:1,000 dilution; Sigma-Aldrich), or anti-AnkB antisera (1:60,000 dilution). Detection was by enhanced chemiluminescence (Thermo Fisher Scientific).

Triton X-114 extractions of transfected HEK293 cells were performed as described previously (Reinicke et al., 2005). Both detergent and aqueous phases were precipitated by trichloroacetic acid. After centrifugation, pellets were washed in acetone, resuspended, and then analyzed.

Confocal laser-scanning microscopy. Processing of infected cells for confocal microscopy was performed as we described previously (Price et al., 2009). Polyclonal rabbit anti–*L. pneumophila* antiserum, anti–*L. micdadei*, or anti–*L. longbeachae* was detected by Alexa Fluor 488–conjugated donkey anti–rabbit IgG (Invitrogen). Polyubiquitinated proteins were detected using anti–polyubiquitin FK1 antibody (1:50 dilution; Enzo Life Sciences, Inc.), followed by Alexa Fluor 555–conjugated goat anti–mouse IgM (Invitrogen). Anti–FT-α, anti–RCE-1, and anti-ICMT were obtained from Santa Cruz Biotechnology, Inc. and used at 1:50 dilution. Farnesylation was detected with a rabbit antifarnesyl antibody (1:50 dilution; Abcam) followed by Alexa Fluor 555-conjugated donkey anti–rabbit IgG (Invitrogen). Alexa Fluor–tagged antibodies against mouse IgG were used as secondary antibodies (Invitrogen). The cells were examined with a laser-scanning confocal microscope (FV1000; Olympus) as we described previously (Price et al., 2009). On average, 8–15 0.2-μm serial z sections of each image were captured and stored for further analyses using Photoshop CS3 (Adobe).

Infection of A/J mice with *L. pneumophila*. All animal work in this manuscript has been performed after approval by the University of Louisville Institutional Animal Care and Use Committee, who follows the US federal guidelines for the use and humane handling of animals in research. Female, pathogen-free, 6–8-wk-old A/J mice were used for infection by intratracheal inoculation with 50 μl containing the bacterial dose as we described previously (Santic et al., 2007; Price et al., 2009). Mice were humanely euthanized at various times, the lungs were removed and homogenized, and dilutions were cultured on buffered charcoal yeast extract agar for 72 h as described previously (Santic et al., 2007; Price et al., 2009).

Online supplemental material. Fig. S1 shows that ectopically expressed 3xFlag AnkB localizes to the cell periphery of *D. discoideum*. Fig. S2 shows that farnesylation of the CaaX motif of AnkB by *D. discoideum* anchors it to the cytosolic face of the LCV membrane. Fig. S3 shows that chemical inhibition of farnesyltransferase by FTI-277 suppresses intracellular proliferation of *L. pneumophila*. Fig. S4 shows that chemical inhibition of farnesyltransferase by FTI-277 suppresses the formation of replicative vacuoles by other *Legionella* species. Fig. S5 shows that chemical inhibition of FT-α does not alter trafficking of the LCV. Fig. S6 shows Dot/Icm-dependent colocalization of FT-α to purified LCVs. Table S1 lists putative CaaX motif proteins in other bacterial pathogens. Table S2 lists the primers used in this study. Online supplemental material is available at http://www.jem.org/cgi/content/full/jem.20100771/DC1.

Y. Abu Kwaik is supported by Public Health Service Awards R01AI43965 and R01AI069321 from the National Institute of Allergy and Infectious Diseases and by the commonwealth of Kentucky Research Challenge Trust Fund.

The authors declare no competing financial interests.

Submitted: 20 April 2010
Accepted: 30 June 2010

REFERENCES

Al-Khodor, S., C.T. Price, F. Habyarimana, A. Kalia, and Y. Abu Kwaik. 2008. A Dot/Icm-translocated ankyrin protein of *Legionella pneumophila* is required for intracellular proliferation within human macrophages and protozoa. *Mol. Microbiol.* 70:908–923.

Al-Khodor, S., T. Al-Quadan, and Y. Abu Kwaik. 2010a. Temporal and differential regulation of expression of the eukaryotic-like ankyrin effectors of *L. pneumophila*. *Environ. Microbiol.* In press. doi:10.1111/j.1758-2229.2010.00159.x.

Al-Khodor, S., C.T.D. Price, A. Kalia, and Y. Abu Kwaik. 2010b. Functional diversity of ankyrin repeats in microbial proteins. *Trends Microbiol.* 18:132–139. doi:10.1016/j.tim.2009.11.004

Alli, O.A., S. Zink, N.K. von Lackum, and Y. Abu-Kwaik. 2003. Comparative assessment of virulence traits in *Legionella* spp. *Microbiology*. 149:631–641. doi:10.1099/mic.0.25980-0

Asare, R., and Y. Abu Kwaik. 2007. Early trafficking and intracellular replication of *Legionella longbeachae* within an ER-derived late endosome-like phagosome. *Cell. Microbiol.* 9:1571–1587. doi:10.1111/j.1462-5822.2007.00894.x

Asare, R., M. Santic, I. Gobin, M. Doric, J. Suttles, J.E. Graham, C.D. Price, and Y. Abu Kwaik. 2007. Genetic susceptibility and caspase activation in mouse and human macrophages are distinct for *Legionella longbeachae* and *L. pneumophila*. *Infect. Immun.* 75:1933–1945. doi:10.1128/IAI.00025-07

Bergo, M.O., G.K. Leung, P. Ambroziak, J.C. Otto, P.J. Casey, and S.G. Young. 2000. Targeted inactivation of the isoprenylcysteine carboxyl methyltransferase gene causes mislocalization of K-Ras in mammalian cells. *J. Biol. Chem.* 275:17605–17610. doi:10.1074/jbc.C000079200

Bordier, C. 1981. Phase separation of integral membrane proteins in Triton X-114 solution. *J. Biol. Chem.* 256:1604–1607.

Boucrot, E., C.R. Beuzón, D.W. Holden, J.P. Gorvel, and S. Méresse. 2003. *Salmonella typhimurium* SifA effector protein requires its membrane-anchoring C-terminal hexapeptide for its biological function. *J. Biol. Chem.* 278:14196–14202. doi:10.1074/jbc.M207901200

Boyartchuk, V.L., M.N. Ashby, and J. Rine. 1997. Modulation of Ras and a-factor function by carboxyl-terminal proteolysis. *Science.* 275:1796–1800. doi:10.1126/science.275.5307.1796

Casey, P.J., P.A. Solski, C.J. Der, and J.E. Buss. 1989. p21ras is modified by a farnesyl isoprenoid. *Proc. Natl. Acad. Sci. USA.* 86:8323–8327. doi:10.1073/pnas.86.21.8323

Dai, Q., E. Choy, V. Chiu, J. Romano, S.R. Slivka, S.A. Steitz, S. Michaelis, and M.R. Philips. 1998. Mammalian prenylcysteine carboxyl methyltransferase is in the endoplasmic reticulum. *J. Biol. Chem.* 273:15030–15034. doi:10.1074/jbc.273.24.15030

de Felipe, K.S., R.T. Glover, X. Charpentier, O.R. Anderson, M. Reyes, C.D. Pericone, and H.A. Shuman. 2008. *Legionella* eukaryotic-like type IV substrates interfere with organelle trafficking. *PLoS Pathog.* 4:e1000117. doi:10.1371/journal.ppat.1000117

Dorer, M.S., D. Kirton, J.S. Bader, and R.R. Isberg. 2006. RNA interference analysis of *Legionella* in *Drosophila* cells: exploitation of early secretory apparatus dynamics. *PLoS Pathog.* 2:e34. doi:10.1371/journal.ppat.0020034

Franco, I.S., H.A. Shuman, and X. Charpentier. 2009. The perplexing functions and surprising origins of *Legionella pneumophila* type IV secretion effectors. *Cell. Microbiol.* 11:1435–1443. doi:10.1111/j.1462-5822.2009.01351.x

Habyarimana, F., S. Al-Khodor, A. Kalia, J.E. Graham, C.T. Price, M.T. Garcia, and Y.A. Kwaik. 2008. Role for the Ankyrin eukaryotic-like genes of *Legionella pneumophila* in parasitism of protozoan hosts and human macrophages. *Environ. Microbiol.* 10:1460–1474. doi:10.1111/j.1462-2920.2007.01560.x

Hancock, J.F., A.I. Magee, J.E. Childs, and C.J. Marshall. 1989. All ras proteins are polyisoprenylated but only some are palmitoylated. *Cell.* 57:1167–1177. doi:10.1016/0092-8674(89)90054-8

Isberg, R.R., T.J. O'Connor, and M. Heidtman. 2009. The *Legionella pneumophila* replication vacuole: making a cosy niche inside host cells. *Nat. Rev. Microbiol.* 7:13–24. doi:10.1038/nrmicro1967

Kagan, J.C., and C.R. Roy. 2002. *Legionella* phagosomes intercept vesicular traffic from endoplasmic reticulum exit sites. *Nat. Cell Biol.* 4:945–954. doi:10.1038/ncb883

Lerner, E.C., Y. Qian, M.A. Blaskovich, R.D. Fossum, A. Vogt, J. Sun, A.D. Cox, C.J. Der, A.D. Hamilton, and S.M. Sebti. 1995. Ras CAAX peptidomimetic FTI-277 selectively blocks oncogenic Ras signaling by inducing cytoplasmic accumulation of inactive Ras-Raf complexes. *J. Biol. Chem.* 270:26802–26806. doi:10.1074/jbc.270.45.26802

Luo, Z.Q., and R.R. Isberg. 2004. Multiple substrates of the *Legionella pneumophila* Dot/Icm system identified by interbacterial protein transfer. *Proc. Natl. Acad. Sci. USA.* 101:841–846. doi:10.1073/pnas.0304916101

McGuire, T.F., Y. Qian, A. Vogt, A.D. Hamilton, and S.M. Sebti. 1996. Platelet-derived growth factor receptor tyrosine phosphorylation requires protein geranylgeranylation but not farnesylation. *J. Biol. Chem.* 271:27402–27407. doi:10.1074/jbc.271.44.27402

Molmeret, M., M. Horn, M. Wagner, M. Santic, and Y. Abu Kwaik. 2005. Amoebae as training grounds for intracellular bacterial pathogens. *Appl. Environ. Microbiol.* 71:20–28. doi:10.1128/AEM.71.1.20-28.2005

Moores, S.L., M.D. Schaber, S.D. Mosser, E. Rands, M.B. O'Hara, V.M. Garsky, M.S. Marshall, D.L. Pompliano, and J.B. Gibbs. 1991. Sequence dependence of protein isoprenylation. *J. Biol. Chem.* 266:14603–14610.

Mumby, S.M., P.J. Casey, A.G. Gilman, S. Gutowski, and P.C. Sternweis. 1990. G protein gamma subunits contain a 20-carbon isoprenoid. *Proc. Natl. Acad. Sci. USA.* 87:5873–5877. doi:10.1073/pnas.87.15.5873

Pang, K.M., M.A. Lynes, and D.A. Knecht. 1999. Variables controlling the expression level of exogenous genes in *Dictyostelium*. *Plasmid.* 41:187–197. doi:10.1006/plas.1999.1391

Price, C.T., S. Al-Khodor, T. Al-Quadan, M. Santic, F. Habyarimana, A. Kalia, and Y.A. Kwaik. 2009. Molecular mimicry by an F-box effector of *Legionella pneumophila* hijacks a conserved polyubiquitination machinery within macrophages and protozoa. *PLoS Pathog.* 5:e1000704. doi:10.1371/journal.ppat.1000704

Price, C.T., S. Al-Khodor, T. Al-Quadan, and Y. Abu Kwaik. 2010. Indispensable role for the eukaryotic-like ankyrin domains of the ankyrin B effector of *Legionella pneumophila* within macrophages and amoebae. *Infect. Immun.* 78:2079–2088. doi:10.1128/IAI.01450-09

Reinicke, A.T., J.L. Hutchinson, A.I. Magee, P. Mastroeni, J. Trowsdale, and A.P. Kelly. 2005. A *Salmonella typhimurium* effector protein SifA is modified by host cell prenylation and S-acylation machinery. *J. Biol. Chem.* 280:14620–14627. doi:10.1074/jbc.M500076200

Reiss, Y., J.L. Goldstein, M.C. Seabra, P.J. Casey, and M.S. Brown. 1990. Inhibition of purified p21ras farnesyl:protein transferase by Cys-AAX tetrapeptides. *Cell.* 62:81–88. doi:10.1016/0092-8674(90)90242-7

Santic, M., R. Asare, M. Doric, and Y. Abu Kwaik. 2007. Host-dependent trigger of caspases and apoptosis by *Legionella pneumophila*. *Infect. Immun.* 75:2903–2913. doi:10.1128/IAI.00147-07

Segal, G., M. Purcell, and H.A. Shuman. 1998. Host cell killing and bacterial conjugation require overlapping sets of genes within a 22-kb region of the *Legionella pneumophila* genome. *Proc. Natl. Acad. Sci. USA.* 95:1669–1674. doi:10.1073/pnas.95.4.1669

Shin, S., and C.R. Roy. 2008. Host cell processes that influence the intracellular survival of *Legionella pneumophila*. *Cell. Microbiol.* 10:1209–1220. doi:10.1111/j.1462-5822.2008.01145.x

Sory, M.P., and G.R. Cornelis. 1994. Translocation of a hybrid YopE-adenylate cyclase from Yersinia enterocolitica into HeLa cells. *Mol. Microbiol.* 14:583–594. doi:10.1111/j.1365-2958.1994.tb02191.x

Tilney, L.G., O.S. Harb, P.S. Connelly, C.G. Robinson, and C.R. Roy. 2001. How the parasitic bacterium *Legionella pneumophila* modifies its phagosome and transforms it into rough ER: implications for conversion of plasma membrane to the ER membrane. *J. Cell Sci.* 114:4637–4650.

Vogel, J.P., H.L. Andrews, S.K. Wong, and R.R. Isberg. 1998. Conjugative transfer by the virulence system of *Legionella pneumophila*. *Science.* 279:873–876. doi:10.1126/science.279.5352.873

Wang, P.C., A. Vancura, T.G. Mitcheson, and J. Kuret. 1992. Two genes in *Saccharomyces cerevisiae* encode a membrane-bound form of casein kinase-1. *Mol. Biol. Cell.* 3:275–286.

Wright, L.P., and M.R. Philips. 2006. Thematic review series: lipid post-translational modifications. CAAX modification and membrane targeting of Ras. *J. Lipid Res.* 47:883–891. doi:10.1194/jlr.R600004-JLR200

Yamane, H.K., C.C. Farnsworth, H.Y. Xie, W. Howald, B.K. Fung, S. Clarke, M.H. Gelb, and J.A. Glomset. 1990. Brain G protein gamma subunits contain an all-trans-geranylgeranylcysteine methyl ester at their carboxyl termini. *Proc. Natl. Acad. Sci. USA.* 87:5868–5872. doi:10.1073/pnas.87.15.5868